

Structural and microwave dielectric behavior of $(\text{Li}_{1/4}\text{Nb}_{3/4})$ substituted $\text{Zr}_x\text{Sn}_y\text{Ti}_z\text{O}_4$ ($x + y + z = 2$) system

Li-Xia Pang^{a,b,*}, Di Zhou^b, Yue-Hua Chen^b, Hong Wang^b

^a Laboratory of Thin Film Techniques and Optical Test, Xi'an Technological University, Xi'an 710032, China

^b Electronic Materials Research Laboratory, Key Laboratory of the Ministry of Education, Xi'an Jiaotong University, Xi'an 710049, China

ARTICLE INFO

Article history:

Received 17 May 2010

Received in revised form 17 August 2010

Accepted 1 October 2010

Keywords:

Ceramics
Electronic materials
Sintering
Dielectric properties

ABSTRACT

The phase structure, microwave dielectric properties, and their stability with different annealing conditions have been investigated in $(\text{Li}_{1/4}\text{Nb}_{3/4})$ substituted $\text{Zr}_x\text{Sn}_y\text{Ti}_z\text{O}_4$ system. The sintering temperature of $\text{Zr}_x\text{Sn}_y\text{Ti}_z\text{O}_4$ ceramic was lowered from 1500 to 1140 °C by $(\text{Li}_{1/4}\text{Nb}_{3/4})$ substitution. Both X-ray diffraction (XRD) analysis and electron diffraction (ED) analysis revealed that the $(\text{Li}_{1/4}\text{Nb}_{3/4})$ substituted $\text{Zr}_x\text{Sn}_y\text{Ti}_z\text{O}_4$ ceramic crystallized as the high-temperature disordered ZrTiO_4 phase. As the content of Sn increased from 0.10 to 0.30, the permittivity of the $(\text{Zr}_{1-x}\text{Sn}_x)(\text{Li}_{1/4}\text{Nb}_{3/4})_{0.4}\text{Ti}_{0.6}\text{O}_4$ ceramic decreased gradually from 35.5 to 31.5, the Q_f value increased from 37,800 to 58,300 GHz, and TCF value shifted slightly from -4.5 to -33.0 ppm °C⁻¹. Both the phase structure and microwave dielectric properties of $(\text{Zr}_{1-x}\text{Sn}_x)(\text{Li}_{1/4}\text{Nb}_{3/4})_{0.4}\text{Ti}_{0.6}\text{O}_4$ ceramics were stable with annealing conditions.

© 2010 Elsevier B.V. All rights reserved.

1. Introduction

The proliferation of commercial wireless technologies, such as cellular phones and global positioning systems, has been making rapid progress due to the improved performance of dielectric resonators at microwave frequencies. Requirements for these dielectric resonators combine a high dielectric constant ($\epsilon_r > 25$) for possible size miniaturization (the size of a dielectric resonator $\propto 1/\epsilon_r$), a high quality factor ($Q_f > 5000$, where $Q_f = 1/\tan \delta$), and a near-zero temperature coefficient of resonant frequency (TCF) for temperature stable circuits [1]. In recent years, ZrTiO_4 ceramics have attracted much interest due to their specific electrical and structural properties [2–5], and zirconium titanate-based ceramics have been in use as temperature-stable dielectric materials for ceramic capacitors for a long time. More recently they have played an important role in applications as stable oscillators at microwave frequencies used in satellite communication such as cell phones and navigation satellite timing and ranging global position system (GPS). The industrial use of ZrTiO_4 motivated numerous studies of its structure, stability, and various physical properties [6–8]. However, the ZrTiO_4 ceramic is difficult to be fired below 1450 °C. On the other hand, ZrTiO_4 is known to undergo an ordering transition at 1120–1200 °C [9] and the ordered ZrTiO_4 pos-

sesses a lower dielectric constant [6]. Sn substitution for Zr (Ti) improved the densification behavior in ZrTiO_4 system and it was clearly effective in suppressing the driving force for the long-range cation-ordering reaction [8]. Meanwhile, Sn substitution enlarged the solid solubility of ZrO_2 – TiO_2 system [2], which was benefit to get the needed dielectric properties by adjusting the composition. ZrTiO_4 with 20 mol% Zr replaced by Sn ion showed excellent microwave dielectric properties with $\epsilon_r = 38$, $Q_f = 8000$ at 7 GHz and $\text{TCF} = 0$ ppm °C⁻¹ [10,11]. However, the sintering temperature of $\text{Zr}_x\text{Sn}_y\text{Ti}_z\text{O}_4$ was still very high (above 1500 °C) and difficult to be lowered to below 1300 °C without the great deterioration on microwave dielectric properties. Our previous work [12] showed that 40 mol% $(\text{Li}_{1/4}\text{Nb}_{3/4})$ substitution in ZrTiO_4 system had successfully lowered the sintering temperature to about 1140 °C. However, a phase transition from the high-temperature disordered phase to the 5:7 ordered phase occurred when the Zr was substituted by $(\text{Li}_{1/4}\text{Nb}_{3/4})$. In this work, 40 mol% $(\text{Li}_{1/4}\text{Nb}_{3/4})$ was used to substitute for Ti in ZrTiO_4 system to lower the sintering temperature. At the same time, Sn substitution for Zr was applied to tailor the microwave dielectric properties. $(\text{Zr}_{1-x}\text{Sn}_x)(\text{Li}_{1/4}\text{Nb}_{3/4})_{0.4}\text{Ti}_{0.6}\text{O}_4$ ($x = 0.10, 0.15, 0.20, 0.30$) ceramics were prepared by conventional solid state reaction method. The phase structure, microwave dielectric properties, and stability with different annealing conditions were studied.

2. Experimental

The compositions of $(\text{Zr}_{1-x}\text{Sn}_x)(\text{Li}_{1/4}\text{Nb}_{3/4})_{0.4}\text{Ti}_{0.6}\text{O}_4$ ($x = 0.10, 0.15, 0.20, 0.30$) were prepared by conventional solid state reaction method using high purity reagent-grade raw materials of Li_2CO_3 (>99%, Guo-Yao Co., Ltd., Shanghai, China),

* Corresponding author at: Laboratory of Thin Film Techniques and Optical Test, Xi'an Technological University, Xi'an 710032, China. Tel.: +86 29 83208006; fax: +86 29 83208210.

E-mail address: plx1982@gmail.com (L.-X. Pang).

Table 1
Lattice parameters and microwave dielectric properties of $(Zr_{1-x}Sn_x)(Li_{1/4}Nb_{3/4})_{0.4}Ti_{0.6}O_4$ ceramics with different annealing conditions.

Samples	Annealing condition ($^{\circ}C h^{-1}$)	Lattice parameter (\AA)			ϵ_r	Q_f (kHz)	TCF ($\text{ppm } ^{\circ}C^{-1}$)
		a	b	c			
$x=0.10$	120	4.833	5.525	5.074	35.53 ± 0.28	37.8 ± 0.6	-4.5 ± 1.5
$x=0.15$	120	4.817	5.539	5.071	34.36 ± 0.21	44.5 ± 0.7	-14.3 ± 2.1
$x=0.20$	120	4.808	5.562	5.076	32.65 ± 0.18	47.9 ± 0.6	-22.1 ± 1.4
$x=0.30$	120	4.785	5.584	5.076	31.82 ± 0.15	58.3 ± 0.6	-33.0 ± 2.5
$x=0.10$	5	4.830	5.527	5.072	35.07 ± 0.21	36.9 ± 0.5	-9.5 ± 1.2
$x=0.20$	5	4.805	5.561	5.073	32.36 ± 0.17	50.3 ± 0.5	-23.9 ± 2.2

Nb_2O_5 (>99%, Zhu-Zhou Harden Alloys Co., Ltd., Zhuzhou, China), rutile TiO_2 (>99%, Linghua Co., Ltd., Zhaoqing, China), ZrO_2 (>99.5%, Xinxing Co., Ltd., Yixing, China) and SnO_2 (>99.5%, Xinxing Co., Ltd., Yixing, China). The raw materials were weighted according to the compositions and ball milled. The mixtures were calcined at 950–1000 $^{\circ}C$ for 5 h and then re-milled for 5 h. The milled powders were dried and granulated with PVA binder and pressed into cylinders (10 mm in diameter and 5 mm in height) under a uniaxial pressure of 200 MPa. The cylinders were sintered in air at 1110–1250 $^{\circ}C$ for 3 h and cooled at the rate of 120 and 5 $^{\circ}C h^{-1}$ respectively.

The crystalline phases of the samples were investigated using an X-ray diffractometry with $Cu K\alpha$ radiation (Rigaku D/MAX-2400 X-ray diffractometry, Tokyo, Japan). The microstructures of the fractured surfaces of $(Zr_{1-x}Sn_x)(Li_{1/4}Nb_{3/4})_{0.4}Ti_{0.6}O_4$ ceramics were observed by scanning electron microscopy (SEM) (JSM-6360LV, JEOL, Tokyo, Japan). For transmission electron microscopy (TEM), the sintered ceramics were crushed into grains, screened and ground again in an agate mortar and pestle. The final powders were then deposited on a carbon-coated copper grid. AJEM-3010 transmission electron microscope (JEM-3010, JEOL, Tokyo, Japan) was used for electron diffraction studies. The dielectric behaviors at microwave frequency of the samples were measured by the TE_{018} shielded cavity method [13] with a network analyzer (8720ES, Agilent, Palo Alto, CA, USA) and a temperature chamber (DELTA 9023, Delta Design, Poway, CA, USA). The TCF was calculated by the following formula:

$$TCF = \frac{f_{85} - f_{25}}{f_{25}(85 - 25)} \times 10^6 \text{ (ppm } ^{\circ}C^{-1}) \quad (1)$$

where f_{85} and f_{25} were the TE_{018} resonant frequencies at 85 and 25 $^{\circ}C$, respectively.

3. Results and discussion

The XRD patterns of powders of $(Zr_{1-x}Sn_x)(Li_{1/4}Nb_{3/4})_{0.4}Ti_{0.6}O_4$ ($x=0.10, 0.15, 0.20, 0.30$) ceramics cooled at the rate of 120 $^{\circ}C h^{-1}$ are shown in Fig. 1. All of them can be fully indexed as a single-phase of $ZrTiO_4$ (JCPDS card No. 74-1504). With the Sn content increasing, the diffraction peaks (002)/(120) and (113)/(222) split respectively, and the (031) peak moved to smaller diffraction angle. The structural parameters are calculated and presented in Table 1. It shows that as the content of Sn increased, the lattice parameter a decreased and b increased greatly. Wolfram and Göbel [2] suggested that the approach of $ZrTiO_4$ lattice toward the rutile structure was responsible for the opposite change of the lattice parameters in $(Zr_{1-x}Sn_xTi)_4O_4$ system. By the tendency to straighten

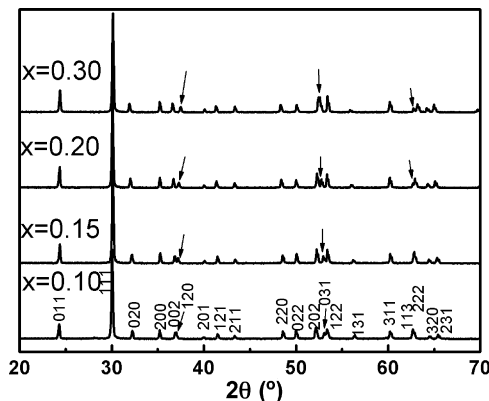


Fig. 1. XRD patterns for powders of $(Zr_{1-x}Sn_x)(Li_{1/4}Nb_{3/4})_{0.4}Ti_{0.6}O_4$ ceramics cooled at 120 $^{\circ}C h^{-1}$.

out the zig-zag lines of octahedral the lattice is contracted along the a axis and dilated in the b direction.

Fig. 2 shows the relative densities of $(Zr_{1-x}Sn_x)(Li_{1/4}Nb_{3/4})_{0.4}Ti_{0.6}O_4$ ceramics as a function of sintering temperature. For all $(Zr_{1-x}Sn_x)(Li_{1/4}Nb_{3/4})_{0.4}Ti_{0.6}O_4$ ceramics, the relative density got above 97% at 1140 $^{\circ}C$, which means that the sintering temperature of $(Zr_{1-x}Sn_x)TiO_4$ could also be lowered to 1140 $^{\circ}C$ by 40 mol% Ti being replaced by $(Li_{1/4}Nb_{3/4})$. On the other hand, it was seen from Fig. 2 that with the sintering temperature increasing further to above 1200 $^{\circ}C$, the relative density of $(Zr_{1-x}Sn_x)(Li_{1/4}Nb_{3/4})_{0.4}Ti_{0.6}O_4$ decreased lightly when $x=0.10$, and it remained stable when the Sn content increased to 0.15. It suggested that the sintering behavior was improved by increasing Sn content.

Fig. 3 presents the typical scanning electron microscopy (SEM) of fractured surfaces of $(Zr_{1-x}Sn_x)(Li_{1/4}Nb_{3/4})_{0.4}Ti_{0.6}O_4$ ceramics cooled at the rate of 120 $^{\circ}C h^{-1}$. All the specimens sintered at 1140 $^{\circ}C$ showed dense microstructures with grain size between 2 and 3 μm . Comparing Fig. 3(d) with Fig. 3(a), the grain size of $(Zr_{1-x}Sn_x)(Li_{1/4}Nb_{3/4})_{0.4}Ti_{0.6}O_4$ ceramic increased with sintering temperature and remained uniform. The microstructures with uniform grain size might be beneficial to the microwave dielectric properties.

The dielectric constants (ϵ_r) of $(Zr_{1-x}Sn_x)(Li_{1/4}Nb_{3/4})_{0.4}Ti_{0.6}O_4$ ceramics as a function of sintering temperature are shown in Fig. 4(a). The dielectric constants of $(Zr_{1-x}Sn_x)(Li_{1/4}Nb_{3/4})_{0.4}Ti_{0.6}O_4$ ceramics were steady-going in the sintering temperature range between 1140 and 1250 $^{\circ}C$.

The theoretical dielectric constant can be estimated using Clausius–Mossotti (C–M) equation [14] and the calculated values are shown in Table 2:

$$\epsilon_r = \frac{3V_m + 8\pi\alpha_D}{3V_m - 4\pi\alpha_D} \quad (2)$$

where α_D is the total dielectric polarizability and V_m is the molar volume. Usually, the total dielectric polarizability is assumed to be

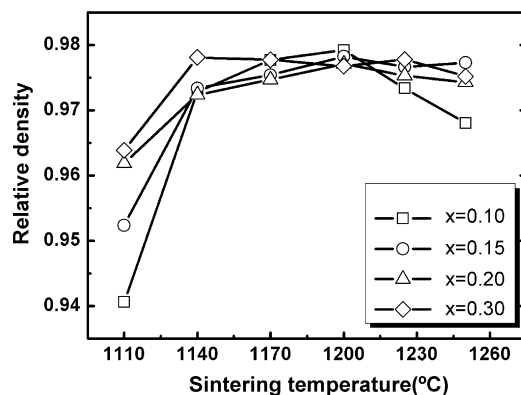


Fig. 2. Dependence of relative density on sintering temperature for $(Zr_{1-x}Sn_x)(Li_{1/4}Nb_{3/4})_{0.4}Ti_{0.6}O_4$ ceramics.

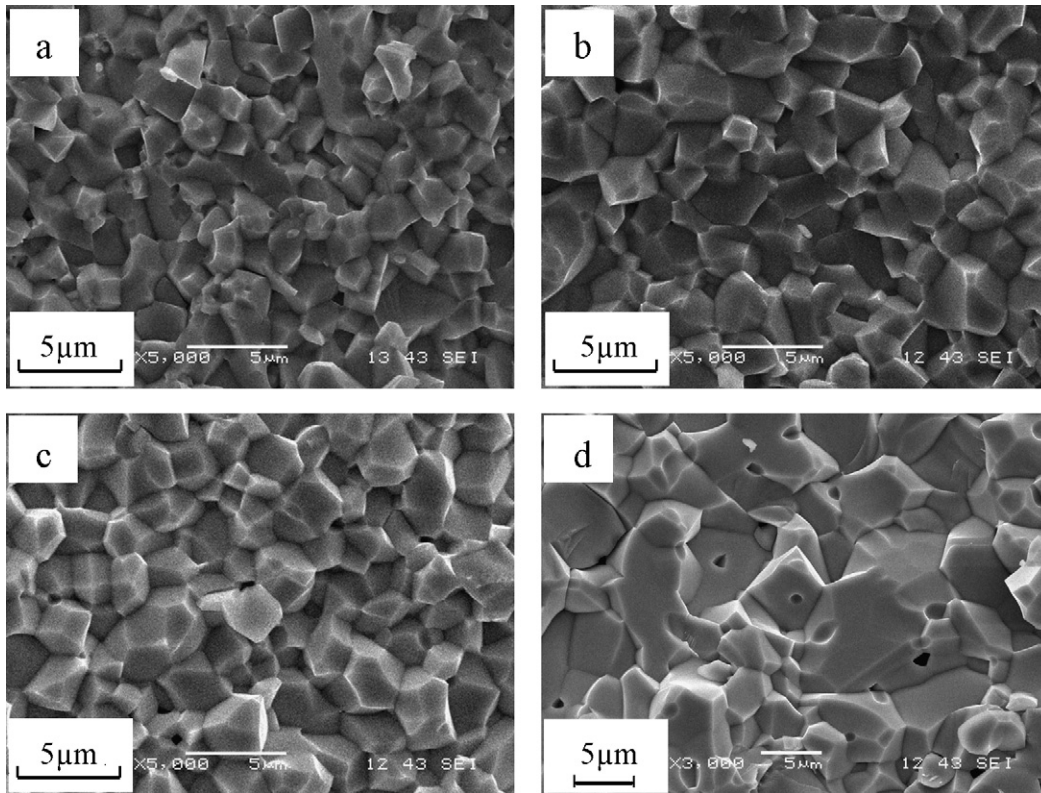


Fig. 3. SEM of fractured surfaces of $(Zr_{1-x}Sn_x)(Li_{1/4}Nb_{3/4})_{0.4}Ti_{0.6}O_4$ ceramics cooled at $120^\circ C h^{-1}$: (a) $x=0.10$, (b) $x=0.20$, (c) $x=0.30$ sintered at $1140^\circ C$, and (d) $x=0.10$ sintered at $1225^\circ C$.

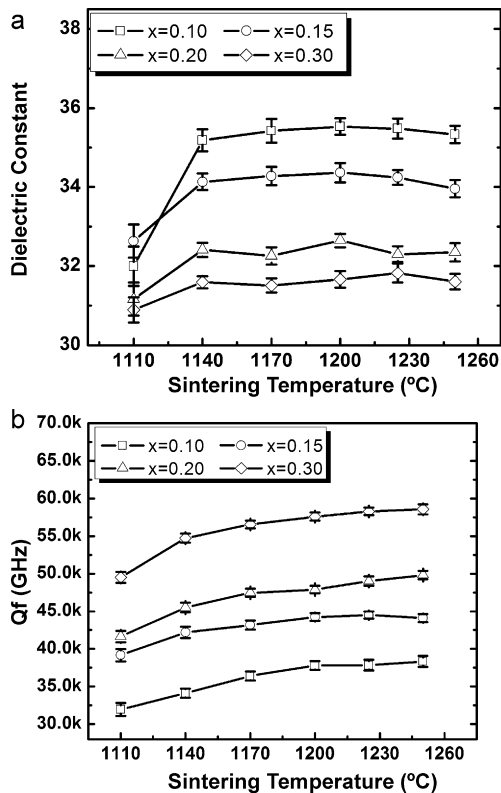


Fig. 4. Microwave dielectric properties of $(Zr_{1-x}Sn_x)(Li_{1/4}Nb_{3/4})_{0.4}Ti_{0.6}O_4$ ceramics cooled at $120^\circ C h^{-1}$: (a) dielectric constant (ϵ_r) and (b) quality factor (Q_f) value as a function of sintering temperature.

equal to the sum of individual ion polarizabilities [15]. As shown in Table 2, the theoretical dielectric constant decreased slightly from 24.15 to 22.83 and the observed value decreased gradually from 35.5 to 31.5 as the content of Sn increased from 0.10 to 0.30, which resulted from the smaller ionic polarizability of Sn^{4+} (2.83 \AA^3) than that of Zr^{4+} (3.25 \AA^3) [15]. On the other hand, the calculated dielectric constants are smaller than the observed ones. According to Shannon's [15] work, the deviation of $\epsilon_{theo.}$ from $\epsilon_{obs.}$ is due to the "rattling" or "compression" effect in the MO_6 (M: cations) octahedron that deviated from ideal octahedron structure. In the $(Zr_{1-x}Sn_x)(Li_{1/4}Nb_{3/4})_{0.4}Ti_{0.6}O_4$ system, the rattling of the small Ti^{4+} cations in TiO_6 octahedra could contribute much more to macroscopic polarizability. As a consequence, the observed polarizabilities are larger than the theoretical ones. On the other hand, Wolfram and Göbel [2] gave an explanation that the high dielectric constant would result from the hybridization of the oxygen p states with the d states of the transition metal ions (Zr^{4+} and Ti^{4+}) in the $(ZrSn)TiO_4$ phase.

The quality factors (Q_f values) of $(Zr_{1-x}Sn_x)(Li_{1/4}Nb_{3/4})_{0.4}Ti_{0.6}O_4$ ceramics increased slightly with sintering temperature increasing, and on the other hand, the Q_f value of $(Zr_{1-x}Sn_x)(Li_{1/4}Nb_{3/4})_{0.4}Ti_{0.6}O_4$ ceramics increased from 37,800 to about 58,300 GHz as the content of Sn increased from 0.10 to 0.30, as shown in Fig. 4(b) and Table 1. Microwave dielectric loss

Table 2
Observed and theoretical dielectric constant (ϵ_r) from C–M equation of the $(Zr_{1-x}Sn_x)(Li_{1/4}Nb_{3/4})_{0.4}Ti_{0.6}O_4$ ceramics.

Samples	$\alpha_D (\text{\AA}^3)$	Unit cell volume (\AA^3) (Z=2)	ϵ_r (cal.)	ϵ_r (obs.)
$x=0.10$	28.634	135.49	24.15	35.53 ± 0.28
$x=0.15$	28.592	135.30	24.13	34.36 ± 0.21
$x=0.20$	28.550	135.74	23.21	32.65 ± 0.18
$x=0.30$	28.466	135.63	22.83	31.82 ± 0.15

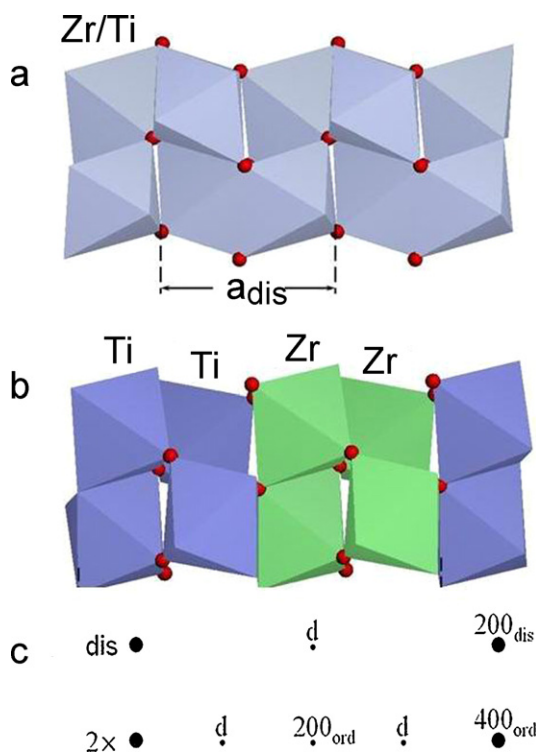


Fig. 5. [010] projection of ZrTiO_4 structures: (a) high temperature disordered phase; (b) the commensurate ordered phase ($2\times$) for low temperature ordered ZrTiO_4 ; (c) schematic of $h00$ systematic row in electron diffraction patterns of disordered ZrTiO_4 form (dis) and $2\times$ commensurate ordered form ($2\times$) (d): double diffraction).

includes two parts: intrinsic loss and extrinsic loss. Intrinsic losses were caused by absorptions of phonon oscillation and extrinsic losses were caused by lattice defect (impurity, cavity, substitution, grain boundaries, size and shapes of grains, second phase, pores, etc.) [16,17]. Considering that Zr^{4+} has larger polarizability than Sn^{4+} [15], especially that the hybridization of the oxygen p states with the d states of Zr^{4+} might occur, it could be concluded that contribution to microwave dielectric constant from ionic displacement polarization of Zr^{4+} was larger than that of Sn^{4+} and oscillation of Zr^{4+} was stronger than that of Sn^{4+} in the same structure and the same atomic position. Hence the substitution of Sn^{4+} increased the Q_f values of $(\text{Zr}_{1-x}\text{Sn}_x)(\text{Li}_{1/4}\text{Nb}_{3/4})_{0.4}\text{Ti}_{0.6}\text{O}_4$ ceramics. The temperature coefficients of resonant frequencies (TCF) of $(\text{Zr}_{1-x}\text{Sn}_x)(\text{Li}_{1/4}\text{Nb}_{3/4})_{0.4}\text{Ti}_{0.6}\text{O}_4$ ceramics are presented in Table 1. As the content of Sn increased from 0.10 to 0.30, the TCF value shifted slightly from -4.5 to -33.0 ppm $^\circ\text{C}^{-1}$.

The stability of phase structures with annealing conditions was studied through electron diffraction (ED) method, as ED method is a good way to study the disorder–order phase transition. It is well known that the high temperature disordered ZrTiO_4 phase crystallizes in orthorhombic $\alpha\text{-PbO}_2$ structure with space group $Pbcn$. Zr and Ti randomly distribute in the octahedral site. For the low temperature ordered ZrTiO_4 phase, two layers of distorted Zr sites and two layers of octahedral Ti sites alternatively stack along the a -axis, which gives rise to a doubling of the cell parameter a . Fig. 5 shows the [010] projection of the high temperature disordered and the low temperature ordered ZrTiO_4 structures, combining with the schematic of $h00$ systematic row in ED patterns [18]. The representative [011] ED pattern of $(\text{Zr}_{1-x}\text{Sn}_x)(\text{Li}_{1/4}\text{Nb}_{3/4})_{0.4}\text{Ti}_{0.6}\text{O}_4$ ($x=0.20$) specimen which was cooled at the rate of 120°C h^{-1} in Fig. 6(a) shows that the $(\text{Zr}_{1-x}\text{Sn}_x)(\text{Li}_{1/4}\text{Nb}_{3/4})_{0.4}\text{Ti}_{0.6}\text{O}_4$ ceramics crystallized as disordered ZrTiO_4 phase when they were sintered at 1140°C , when the disorder–order phase transition would occur

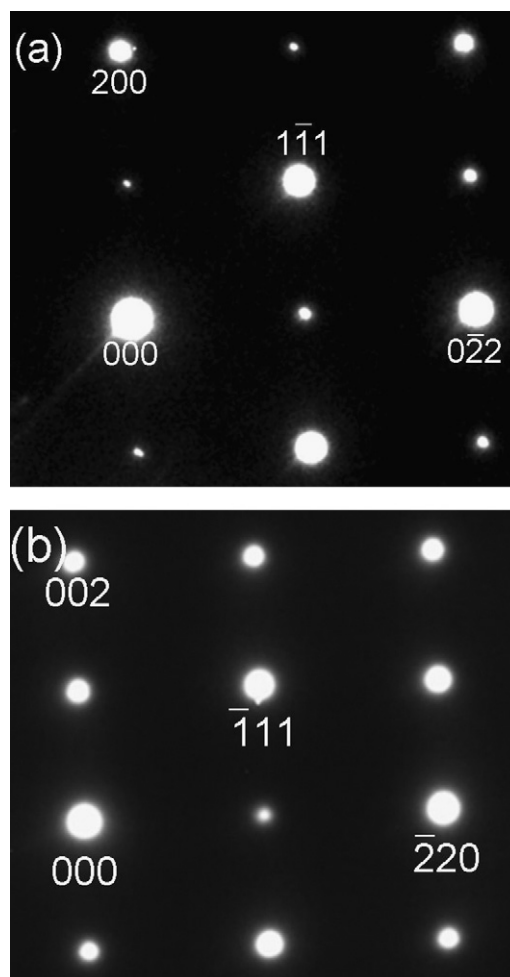


Fig. 6. (a) Representative [011] electron diffraction pattern of $(\text{Zr}_{1-x}\text{Sn}_x)(\text{Li}_{1/4}\text{Nb}_{3/4})_{0.4}\text{Ti}_{0.6}\text{O}_4$ ($x=0.20$) specimen cooled at 120°C h^{-1} ; and (b) representative [110] electron diffraction pattern of $(\text{Zr}_{1-x}\text{Sn}_x)(\text{Li}_{1/4}\text{Nb}_{3/4})_{0.4}\text{Ti}_{0.6}\text{O}_4$ ($x=0.20$) specimen cooled at 5°C h^{-1} .

in pure ZrTiO_4 system [9]. It is known that the phase transition from the high temperature disordered phase to low temperature ordered phase in ZrTiO_4 system is a restricted process and it just could occur at a rate of no higher than 6°C h^{-1} . Fig. 6(b) shows the typical [110] ED pattern of the specimen cooled at the rate of 5°C h^{-1} , and it reveals that the specimen still remains the high temperature disordered phase even cooled at such a low cooling rate. The disorder–order phase transition is successively suppressed in the $(\text{Li}_{1/4}\text{Nb}_{3/4})$ substituted $\text{Zr}_x\text{Sn}_y\text{Ti}_z\text{O}_4$ system. The microwave dielectric properties of the $(\text{Zr}_{1-x}\text{Sn}_x)(\text{Li}_{1/4}\text{Nb}_{3/4})_{0.4}\text{Ti}_{0.6}\text{O}_4$ ($x=0.10$ and 0.20) ceramics cooled at the rate of 5°C h^{-1} were shown in Table 1. It is found that the microwave dielectric properties of the $(\text{Li}_{1/4}\text{Nb}_{3/4})$ substituted $\text{Zr}_x\text{Sn}_y\text{Ti}_z\text{O}_4$ system are also stable with annealing conditions.

4. Conclusions

$(\text{Zr}_{1-x}\text{Sn}_x)(\text{Li}_{1/4}\text{Nb}_{3/4})_{0.4}\text{Ti}_{0.6}\text{O}_4$ ($x=0.10, 0.15, 0.20, 0.30$) ceramics were prepared by conventional solid state reaction method. The phase structure, microwave dielectric properties, and their stability with different annealing processes have been investigated. The sintering temperature has been lowered from 1500 to 1140°C by $(\text{Li}_{1/4}\text{Nb}_{3/4})$ substitution for Ti in $\text{Zr}_x\text{Sn}_y\text{Ti}_z\text{O}_4$ system. XRD and ED analysis showed that the $(\text{Li}_{1/4}\text{Nb}_{3/4})$ substituted $\text{Zr}_x\text{Sn}_y\text{Ti}_z\text{O}_4$ system remained the high temperature disordered

ZrTiO₄ phase. When the Sn content increased from 0.10 to 0.30, the dielectric constant of (Zr_{1-x}Sn_x)(Li_{1/4}Nb_{3/4})_{0.4}Ti_{0.6}O₄ ceramics decreased gradually from 35.5 to 31.5, Q_f value increased from 37,800 to 58,300 GHz, and TCF value shifted slightly from -4.5 to -33.0 ppm °C⁻¹. The low temperature sintering, stable phase structure, and adjustable microwave dielectric properties can be achieved in (Li_{1/4}Nb_{3/4}) substitution Zr_xSn_yTi_zO₄ system. It is a good candidate in wireless communication systems.

Acknowledgements

This work was supported by the National 973-project of China (2009CB623302), NSFC project of China (60871044, 50835007).

References

- [1] T. Takada, S.F. Wang, S. Yoshikawa, S.J. Jang, R.E. Newnham, *J. Am. Ceram. Soc.* 77 (1994) 1909.
- [2] G. Wolfram, E. Göbel, *Mater. Res. Bull.* 16 (1981) 1455.
- [3] S.X. Zhang, J.B. Li, J. Cao, H.Z. Zhai, B. Zhang, *J. Mater. Sci. Lett.* 20 (2001) 1409.
- [4] Y.K. Kim, H.M. Jang, *J. Appl. Phys.* 89 (2001) 6349.
- [5] J. Macan, Gajović, F. A., H. Ivanković, *J. Eur. Ceram. Soc.* 29 (2009) 691.
- [6] F. Azough, R. Freer, C.L. Wang, G.W. Lorimer, *J. Mater. Sci.* 31 (1996) 2539.
- [7] C.L. Wang, H.Y. Lee, F. Azough, R. Freer, *J. Mater. Sci.* 32 (1997) 1693.
- [8] R. Christofferen, P.K. Davies, X.H. Wei, *J. Am. Ceram. Soc.* 77 (1994) 1441.
- [9] A.E. McHale, R.S. Roth, *J. Am. Ceram. Soc.* 66 (1983) 18.
- [10] Y. Higuchi, H. Katsube, US patent 4665041 (1987).
- [11] Y. Park, N.H. Cho, Y.H. Kim, US patent 5432134 (1995).
- [12] L.X. Pang, H. Wang, D. Zhou, X. Yao, *Jpn. J. Appl. Phys.* 48 (2009) 051403.
- [13] J. Krupka, K. Derzakowski, B. Riddle, J. Baker-Jarvis, *Meas. Sci. Technol.* 9 (1998) 1751.
- [14] E.E. Havinga, *J. Phys. Chem. Solids* 18 (1961) 253.
- [15] R.D. Shannon, *J. Appl. Phys.* 73 (1993) 348.
- [16] S.J. Penn, N.M. Alford, A. Templeton, X. Wang, M. Xu, M. Reece, K. Schrapel, *J. Am. Ceram. Soc.* 80 (1997) 1885.
- [17] H. Tamura, *Am. Ceram. Soc. Bull.* 73 (1994) 92.
- [18] R. Christoffersen, P.K. Davies, *J. Am. Ceram. Soc.* 75 (1992) 563.